Domain Aggregation Networks for Multi-Source Domain Adaptation

Junfeng Wen [1] **Russ Greiner** [1] **Dale Schuurmans** [1 2]

Abstract

In many real-world applications, we want to exploit multiple source datasets to build a model for a different but related target dataset. Despite the recent empirical success, most existing research has used ad-hoc methods to combine multiple sources, leading to a gap between theory and practice. In this paper, we develop a finite-sample generalization bound based on domain discrepancy and accordingly propose a theoretically justified optimization procedure. Our algorithm, Domain AggRegation Network (DARN), can automatically and dynamically balance between including more data to increase effective sample size and excluding irrelevant data to avoid negative effects during training. We find that DARN can significantly outperform the state-of-the-art alternatives on multiple real-world tasks, including digit/object recognition and sentiment analysis.

1. Introduction

Many machine learning algorithms assume the learned predictor will be tested on the data from the same distribution as the training data. This assumption, although reasonable, is not necessarily true for many real-world applications. For example, patients from one hospital may have a different distribution of gender, height and weight from another hospital. Consequently, a diagnostic model constructed at one location may not be directly applicable to another location without proper adjustment. The situation becomes even more challenging when we want to use data from multiple *source domains* to build a model for a *target domain*, as this requires deciding, e.g., how to select the relevant source domains and how to effectively aggregate these domains when training complex models like neural networks. Including irrelevant data from certain source domains can severely reduce the performance on the target domain.

[1]Department of Computing Science, University of Alberta, Edmonton, Canada [2]Google Brain. Correspondence to: Junfeng Wen <junfengwen@gmail.com>.

Proceedings of the 37^{th} International Conference on Machine Learning, Vienna, Austria, PMLR 119, 2020.

To address this problem, researchers have been exploring methods of *transfer learning* (Pan & Yang, 2009) or *domain adaptation* (Mansour et al., 2009a; Cortes et al., 2019), where a model is trained based on labelled source data and unlabelled target data. Most existing works have focused on single-source to single-target ("one-to-one") domain adaptation, using different assumptions such as covariate shift (Shimodaira, 2000; Gretton et al., 2009; Sugiyama & Kawanabe, 2012) or concept drift (Jiang & Zhai, 2007; Gama et al., 2014). When dealing with multiple source domains, one may attempt to directly use these approaches by combining all source data into a large joint dataset and then apply one-to-one adaptation. This naïve aggregation method will often fail as not all source domains are equally important when transferring to a specific target domain. There are some works on multi-source to single-target adaptation. Although some of them are theoretically motivated with cross-domain generalization bounds, they either use ad-hoc aggregation rules when developing practical algorithms (Zhao et al., 2018; Li et al., 2018) or lack finite-sample analysis (Mansour et al., 2009b;c; Hoffman et al., 2018a). This leaves a gap between the theory for multi-source adaptation and practical algorithm for domain aggregation.

This research has three contributions: First, we develop a finite-sample cross-domain generalization bound for multi-source adaptation, which is based on the discrepancy introduced by Cortes et al. (2019). We show that in order to improve performance on the specific target domain, there is a trade-off between including all source domains to increase effective sample size, versus excluding less relevant source domains to avoid negative outcomes. Second, motivated by our theory and domain adversarial method (Ganin & Lempitsky, 2015; Ganin et al., 2016), we propose Domain AggRegation Network (DARN), which can dynamically adjust the importance weights of the source domains during the course of training. Unlike previous works, our aggregation scheme (Eq. (7)), which itself is of independent interest in some other contexts, is a direct optimization of our generalization upper bound (Eq. (4)) without resorting to surrogates. Third, our experiments on digit/object recognition and sentiment analysis show that DARN can significantly outperform state-of-the-art methods.

This paper is organized as follows. Section 2 introduces necessary background on one-to-one adaptation based on

discrepancy. Section 3 elaborates our theoretical analysis and the corresponding algorithm deployment. Section 4 discusses about related approaches in the literature, highlighting the key differences to our method. Section 5 empirically compares the performance of the proposed method to other alternatives. Finally, Section 6 concludes this work.

2. Background on Cross-domain Generalization

This section provides background from previous work on one-to-one domain adaptation (Cortes et al., 2019). Let $\mathcal{X}$ be the input space, $\mathcal{Y} \subseteq \mathbb{R}$ be output space and $\mathcal{H} \subseteq \{h : \mathcal{X} \mapsto \mathcal{Y}\}$ be a hypothesis class. A loss function $L : \mathcal{Y} \times \mathcal{Y} \mapsto \mathbb{R}^+$ is μ-admissible[1] if

$$\forall y, y', y'' \in \mathcal{Y} \quad |L(y', y) - L(y'', y)| \leq \mu\,|y' - y''|. \quad (1)$$

The *discrepancy* (Mansour et al., 2009a) between two distributions P, Q over $\mathcal{X}$ is defined as

$$\begin{aligned} \mathrm{disc}(P, Q) &= \max_{h, h' \in \mathcal{H}} |\mathcal{L}_P(h, h') - \mathcal{L}_Q(h, h')| \\ \text{where} \quad \mathcal{L}_P(h, h') &= \mathbb{E}_{x \sim P}[L(h(x), h'(x))]. \end{aligned} \quad (2)$$

This quantity can be computed or approximated empirically given samples from both distributions. For classification problems with 0-1 loss, it reduces to the well-known $d_{\mathcal{A}}$-distance (Kifer et al., 2004; Blitzer et al., 2008; Ben-David et al., 2010a) and can be approximated using a domain-classifier loss w.r.t. $\mathcal{H}$ (Zhao et al., 2018; Ben-David et al., 2007, Sec.4), while for regression problems with L_2 loss, it reduces to the maximum eigenvalue (Cortes & Mohri, 2011, Sec.5); see Section 3.2 for more details. For two domains $(P, f_P), (Q, f_Q)$ where $f_P, f_Q : \mathcal{X} \mapsto \mathcal{Y}$ are the corresponding labeling functions, we have the following cross-domain generalization bound:

Theorem 1 (Proposition 5 & 8, Cortes et al. (2019)) *Let $\mathfrak{R}_m(\mathcal{H})$ be the Rademacher complexity of $\mathcal{H}$ given sample size m, $\mathcal{H}_Q = \{x \mapsto L(\, h(x),\ f_Q(x)\,) : h \in \mathcal{H}\}$ be the set of functions mapping x to its loss w.r.t. f_Q and $\mathcal{H}$,*

$$\begin{aligned} \eta_{\mathcal{H}} = \mu \times \min_{h \in \mathcal{H}} \big(&\max_{x \in \mathrm{supp}(\widehat{P})} |f_P(x) - h(x)| \\ &+ \max_{x \in \mathrm{supp}(\widehat{Q})} |f_Q(x) - h(x)| \big), \end{aligned} \quad (3)$$

be a constant measuring how well $\mathcal{H}$ can fit the true models where $\mathrm{supp}(\widehat{P})$ is the support of the empirical distribution $\widehat{P}$ (using the μ from Eq. (1)), and $M_Q = \sup_{x \in \mathcal{X}, h \in \mathcal{H}} L(\, h(x),\ f_Q(x)\,)$ be the upper bound on loss for Q. Given $\widehat{Q}$ with m points sampled iid from Q labelled according to f_Q, for $\delta \in (0, 1), \forall h \in \mathcal{H}$, w.p. at least $1 - \delta$,

$$\begin{aligned} \mathcal{L}_P(h, f_P) \leq\ & \mathcal{L}_{\widehat{Q}}(h, f_Q) + \mathrm{disc}(P, Q) + \\ & 2\mathfrak{R}_m(\mathcal{H}_Q) + \eta_{\mathcal{H}} + M_Q \sqrt{\frac{\log(1/\delta)}{2m}}. \end{aligned}$$

This theorem provides a way to generalize across domains when we have sample $\widehat{Q}$ labelled according to f_Q and an unlabelled sample $\widehat{P}$. The first term is the usual loss function for the sample $\widehat{Q}$, while the second term $\mathrm{disc}(P, Q)$ can be estimated based on the unlabelled data $\widehat{Q}, \widehat{P}$. $\eta_{\mathcal{H}}$ measures how well the model family $\mathcal{H}$ can fit the examples from the datasets, and it is not controllable once $\mathcal{H}$ is given. The final term, as a function of sample size m, determines the convergence speed.

3. Domain Aggregation Network

3.1. Theory

Suppose we are given k source domains $\{(S_i, f_{S_i}) : i \in [k] \stackrel{\text{def}}{=} \{1, 2, \ldots, k\}\}$ and a target domain (T, f_T) where S_i, T are distributions over $\mathcal{X}$ and $f_{S_i}, f_T : \mathcal{X} \mapsto \mathcal{Y}$ are their respective labelling functions. For simplicity, assume that each sample $\widehat{S}_i$ has m points, drawn iid from S_i and labelled according to f_{S_i}. We are also given m unlabelled points $\widehat{T}$ drawn iid from T. We want to leverage all source domains' information to learn a model $h \in \mathcal{H}$ minimizing $\mathcal{L}_T(h, f_T)$.

One naïve approach could be to combine all the source domains into a large joint dataset and conduct one-to-one adaptation to the target domain using Theorem 1. However, including data from irrelevant or even adversarial domains is likely to jeopardize the performance on the target domain, which is sometimes referred to as *negative transfer* (Pan & Yang, 2009). Moreover, as certain source domains may be more similar or relevant to the target domain than the others, it makes more sense to adjust their importance according to their utilities. We propose to find domain weights $\alpha_i \geq 0$ such that $\sum_{i=1}^k \alpha_i = 1$ to achieve this. Our main theorem below sheds some light on how we should combine the source domains (the proof is provided in Appendix A):

Theorem 2 *Given k source domains datasets $\{(x_j^{(i)}, y_j^{(i)}) : i \in [k], j \in [m]\}$ with m iid examples each where $\widehat{S}_i = \{x_j^{(i)}\}$ and $y_j^{(i)} = f_{S_i}(x_j^{(i)})$, for any $\boldsymbol{\alpha} \in \Delta = \{\boldsymbol{\alpha} : \alpha_i \geq 0, \sum_i \alpha_i = 1\}, \delta \in (0, 1)$, and $\forall h \in \mathcal{H}$, w.p. at least $1 - \delta$*

$$\begin{aligned} \mathcal{L}_T(h, f_T) \leq & \sum_i \alpha_i [\mathcal{L}_{\widehat{S}_i}(h, f_{S_i}) + \mathrm{disc}(T, S_i) \\ & + 2\mathfrak{R}_m(\mathcal{H}_{S_i}) + \eta_{\mathcal{H},i}] + \|\boldsymbol{\alpha}\|_2 M_S \sqrt{\frac{\log(1/\delta)}{2m}}, \end{aligned} \quad (4)$$

[1] For example, the common L_p losses are μ-admissible (Cortes et al., 2019, Lemma 23).

where $\mathcal{H}_{S_i} = \{x \mapsto L(h(x), f_{S_i}(x)) : h \in \mathcal{H}\}$ is the set of functions mapping x to the corresponding loss, $\eta_{\mathcal{H},i}$ is a constant similar to Eq. (3) with $\widehat{Q} = \widehat{S}_i$, $\widehat{P} = \widehat{T}$ and $M_S = \sup_{i\in[k],x\in\mathcal{X},h\in\mathcal{H}} L(h(x), f_{S_i}(x))$ is the upper bound on loss on the source domains.

There are several remarks.

- In the last term of the bound, $m/\|\boldsymbol{\alpha}\|_2^2$ serves as the *effective sample size*. If $\boldsymbol{\alpha}$ is uniform (i.e., $[1/k, \ldots, 1/k]^\top$), the effective sample size is km; if $\boldsymbol{\alpha}$ is one-hot, we effectively only have m points from exactly one domain.
- Let $g_{h,i} \stackrel{\text{def}}{=} \mathcal{L}_{\widehat{S}_i}(h, f_{S_i}) + \text{disc}(T, S_i)$. Small $g_{h,i}$ indicates that we can achieve small loss on domain S_i, and it is similar to the target domain (i.e., small $\text{disc}(T, S_i)$, estimated from $\widehat{T}, \widehat{S}_i$). We may want to emphasize on S_i by setting α_i close to 1, but this will reduce the effective sample size. Therefore, we have to trade-off between the terms in this bound by choosing a proper $\boldsymbol{\alpha}$.
- When S_i and T are only partially overlapped, it might be difficult to find a suitable α_i. In such cases, the discrepancy could be large because the performance gap on the two domains can be big (see Eq. (2)). Then it would be important for the model to learn certain overlapping representations to control the bound. We can also artificially split the source domains into smaller datasets (e.g., by clustering) then apply our method on the finer scale.
- $\mathfrak{R}_m(\mathcal{H}_{S_i})$ determines how expressive the model family $\mathcal{H}$ is w.r.t. the source data S_i. Although it can be estimated from samples (Bartlett & Mendelson, 2002, Theorem 11), the computation is non-trivial for a model family like neural networks. $\eta_{\mathcal{H},i}$ is assumed to be small, which is a necessary condition for success adaptation (Ben-David et al., 2010b, Theorem 2), and estimating $\eta_{\mathcal{H},i}$ is impossible without labelled target data. As removing these two terms does not seem to be empirically significant, the following analysis ignores them for simplicity.

Before we proceed to develop an algorithm based on the theorem, we compare Eq. (4) to existing finite-sample bounds. The bound of Blitzer et al. (2008, Theorem 3) is informative when we have access to a small set of *labelled* target examples. In such cases, we can improve our bound by using this small labelled target set as an additional source domain S_{k+1}. The bound of Zhao et al. (2018, Theorem 2) is based on the $d_{\mathcal{A}}$-distance, which is a special case of disc in our bound. Moreover, Eq. (4) uses sample-based Rademacher complexity, which is generally tighter than other complexity measures such as VC-dimension (Bartlett & Mendelson, 2002; Koltchinskii et al., 2002; Bousquet et al., 2003). Peng et al. (2019, Theorem 1) provide a bound based on binary classification, which depends on the *unknown* target minimizer. In comparison, our bound uses the *attainable* source loss. Moreover, we relate our theorem to the optimization procedure, as we show next.

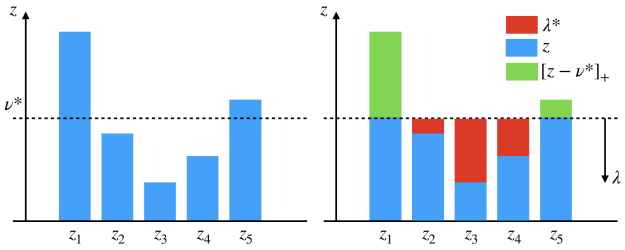

Figure 1: Optimal solution to Eq. (6) (best viewed in color). $\boldsymbol{\lambda}^*$ compensates what is below the ν^*, while ν^* is chosen such that the vector of the green bars has L_2 norm of 1.

3.2. Algorithm

In this section, we develop a practical algorithm, Domain AggRegation Network (DARN), based on Theorem 2. Ignoring the constants, we would like to minimize the upper bound of Eq. (4):

$$\min_{h\in\mathcal{H}} \min_{\boldsymbol{\alpha}\in\Delta} \quad U_h(\boldsymbol{\alpha}) = \langle \mathbf{g}_h, \boldsymbol{\alpha}\rangle + \tau\|\boldsymbol{\alpha}\|_2 \tag{5}$$

where $\mathbf{g}_h = [g_{h,1}, \ldots, g_{h,k}]^\top$ and $\tau > 0$ is a hyper-parameter. If we can solve the inner minimization exactly given h, then we can treat the optimal $\boldsymbol{\alpha}^*(h)$ as a function of h and solve the outer minimization over h effectively. In the following, we show how to achieve this.

Given $\mathbf{g}_h$, the inner minimization can be reformulated as a second-order cone programming problem, but it has no closed-form solution due to the $\tau\|\boldsymbol{\alpha}\|_2$ term. Consider the following problem ($\mathbf{z} = -\mathbf{g}_h/\tau$ recovers the inner minimization):

$$\min_{\boldsymbol{\alpha}\in\Delta} \quad -\langle \mathbf{z}, \boldsymbol{\alpha}\rangle + \|\boldsymbol{\alpha}\|_2 \tag{6}$$

The Lagrangian for its dual problem is

$$\Lambda(\boldsymbol{\alpha}, \boldsymbol{\lambda}, \nu) = -\mathbf{z}^\top\boldsymbol{\alpha} + \|\boldsymbol{\alpha}\|_2 - \boldsymbol{\lambda}^\top\boldsymbol{\alpha} + \nu(\mathbf{1}^\top\boldsymbol{\alpha} - 1),$$

with $\nu \in \mathbb{R}, \boldsymbol{\lambda} \succeq 0$. Taking the derivative w.r.t. $\boldsymbol{\alpha}$ and setting it to zero gives

$$\frac{\partial\Lambda}{\partial\boldsymbol{\alpha}} = -\mathbf{z} + \frac{\boldsymbol{\alpha}}{\|\boldsymbol{\alpha}\|_2} - \boldsymbol{\lambda} + \nu\mathbf{1} = 0 \Rightarrow \frac{\boldsymbol{\alpha}^*}{\|\boldsymbol{\alpha}^*\|_2} = \mathbf{z} - \nu\mathbf{1} + \boldsymbol{\lambda}.$$

Note that $\boldsymbol{\alpha} \neq \mathbf{0}$ so we have the constraint $\|\mathbf{z} - \nu\mathbf{1} + \boldsymbol{\lambda}\|_2 = 1$. Using this $\boldsymbol{\alpha}^*$ in Λ gives the following dual problem

$$\max_{\nu,\boldsymbol{\lambda}} \quad -\nu \qquad \text{s.t.} \quad \|\mathbf{z} - \nu\mathbf{1} + \boldsymbol{\lambda}\|_2 = 1 \quad \text{and} \quad \boldsymbol{\lambda} \succeq 0$$

We would like to *decrease* ν as much as possible, and the best we can attain is the ν^* satisfying $\|[\mathbf{z} - \nu^*\mathbf{1}]_+\|_2 = 1$ where $[\mathbf{v}]_+ = \max(\mathbf{0}, \mathbf{v})$. In this case, the optimal $\boldsymbol{\lambda}^*$ can be attained as $\lambda_i^* = 0$ if $z_i - \nu^* > 0$, otherwise $\lambda_i^* = \nu^* - z_i$; see Fig. 1. Although we do not have a closed-form expression for the optimal ν^*, we can use binary search

to find it, starting from the interval $[z_{\min} - 1, z_{\max}]$ where $z_{\min}, z_{\max}$ are the minimum and maximum of $\mathbf{z}$ respectively. Then we can recover the primal solution as

$$\boldsymbol{\alpha}^* = [\mathbf{z} - \nu^* \mathbf{1}]_+ / \|[\mathbf{z} - \nu^* \mathbf{1}]_+\|_1. \tag{7}$$

Eq. (7) gives rise to a new way to project any vector $\mathbf{z}$ to the probability simplex, which is of independent interest and may be used in some other contexts.[2] It resembles the standard projection onto the simplex based on *squared* Euclidean distance (Duchi et al., 2008, Eq.(3)). One subtle but crucial difference is that Eq. (6) uses $\|\boldsymbol{\alpha}\|_2$ instead of $\|\boldsymbol{\alpha}\|_2^2$. Recall that $\mathbf{z} = -\mathbf{g}_h/\tau$. Here τ can be interpreted as a temperature parameter. On one hand, if $\tau \gg 0$, all $\mathbf{z}$ will have similar values and thus the optimal ν^* will be close to $z_{\max}$ and $\boldsymbol{\alpha}^*$ will be close to uniform. On the other hand, as $\tau \to 0$, $z_{\max}$ will stand out from the rest z_i and eventually $\nu^* = z_{\max} - 1$. This means the $g_{h,i}$ corresponding to the $z_{\max}$ is small enough so we focus solely on this domain and ignore all other domains (even though this will reduce effective sample size as discussed in Section 3.1).

We can optimize our objective and train a neural network h using gradient-based optimizer. The optimal $\boldsymbol{\alpha}^*(h)$ is a function of h and we can backprop through it. To facilitate the gradient computation and show that we can efficiently backprop through the projection of Eq. (7), we derive the Jacobian $J = \partial\boldsymbol{\alpha}/\partial\mathbf{z}$ in Appendix B. This ensures effective end-to-end training.

Now we elaborate on how to compute $g_{h,i}$. The $\mathcal{L}_{\widehat{S}_i}(h, f_{S_i})$ is the task loss. The $\mathrm{disc}(T, S_i)$ depends on whether the task is classification or regression. For classification, disc coincides with the $d_{\mathcal{A}}$-distance, so we use the domain classification loss (Ben-David et al., 2007; Zhao et al., 2018):

$$\mathrm{disc}(\widehat{T}, \widehat{S}_i) = 2\left(1 - \min_{h_d} \widehat{\epsilon}_{T,S_i}(h_d)\right)$$

$$\widehat{\epsilon}_{T,S_i}(h_d) = \frac{1}{2m} \sum_{i=1}^{2m} \left| h_d(x) - \delta_{x \in \widehat{T}} \right|$$

where $\widehat{\epsilon}_{T,S_i}(h_d)$ is the sample domain classification loss of a domain classifier $h_d : \mathcal{X} \mapsto \{0, 1\}$. This minimization over h_d will become maximization once we move it outside of the disc due to the minus sign. Then our objective consists of $\min_h$ and $\max_{h_d}$, which resembles adversarial training (Goodfellow et al., 2014): learning a task classifier h to minimize loss and a domain classifier h_d to maximize domain confusion. More specifically, if we decompose the neural network h into a feature extractor h_{fea} and a label predictor h_y (i.e., $h(x) = (h_y \circ h_{\mathrm{fea}})(x)$), we can learn a domain-classifier h_d on top of h_{fea} to classify $h_{\mathrm{fea}}(x)$ between S_i and T as a binary classification problem, where the domain itself is the label (see Fig. 2). To achieve this, we use the logistic loss to approximate $\widehat{\epsilon}_{T,S_i}(h_d)$ and apply the gradient reversal layer (Ganin & Lempitsky, 2015; Ganin et al., 2016) when optimizing disc through backpropagation.

If we are solving regression problems with L_2 loss, then $\mathrm{disc}(\widehat{T}, \widehat{S}_i) = \|M_T - M_{S_i}\|_2$ is the largest eigenvalue (in magnitude) of the difference of two matrices $M_T = \frac{1}{m}\sum_j h_{\mathrm{fea}}(x_j^{(T)}) h_{\mathrm{fea}}^\top(x_j^{(T)})$ and $M_{S_i} = \frac{1}{m}\sum_j h_{\mathrm{fea}}(x_j^{(i)}) h_{\mathrm{fea}}^\top(x_j^{(i)})$ (Mansour et al., 2009a; Cortes & Mohri, 2011, Sec.5), which can be conveniently approximated using mini-batches and a few steps of power iteration. The overall algorithm is summarized in Algorithm 1.

Algorithm 1 Domain Aggregation Network

Input:

- k labelled source datasets $\{(x_j^{(i)}, y_j^{(i)}) : i \in [k], j \in [m]\}$
- One unlabelled target dataset $\{x_j^{(T)} : j \in [m]\}$
- Temperature parameter $\tau > 0$
- Optimizer learning rate $\eta > 0$

1: Initialize a neural network h with feature extractor h_{fea}, one label prediction head h_y and k domain classification heads $\{h_{d,i} : i \in [k]\}$, as in Fig. 2

2: **repeat**

3: Sample a mini-batch of size B for each dataset

4: Compute the losses for the source mini-batches

$$\widehat{\mathcal{L}}_{S_i}(h) \leftarrow \frac{1}{B}\sum_{j=1}^{B} L\left[(h_y \circ h_{\mathrm{fea}})(x_j^{(i)}),\ y_j^{(i)}\right] \tag{8}$$

5: Compute the sample discrepancies $\widehat{\mathrm{disc}}(T, S_i)$

- If classification, compute as

$$\frac{1}{2B}\sum_{j=1}^{B}\Big[L_d\left((h_{d,i} \circ h_{\mathrm{fea}}^r)(x_j^{(T)}),\ 1\right) + L_d\left((h_{d,i} \circ h_{\mathrm{fea}}^r)(x_j^{(i)}),\ 0\right)\Big] \tag{9}$$

where L_d is the domain classification loss and $h_{\mathrm{fea}}^r = r \circ h_{\mathrm{fea}}$ with r being the GRL

- If regression, compute as

$$\|M_T^r - M_{S_i}^r\|_2 \tag{10}$$

where $M_T^r = \frac{1}{B}\sum_{j=1}^{B} h_{\mathrm{fea}}^r(x_j^{(T)}) h_{\mathrm{fea}}^r(x_j^{(T)})^\top$

and $M_{S_i}^r = \frac{1}{B}\sum_{j=1}^{B} h_{\mathrm{fea}}^r(x_j^{(i)}) h_{\mathrm{fea}}^r(x_j^{(i)})^\top$

6: With $\widehat{g}_{h,i} = \widehat{\mathcal{L}}_{S_i}(h) + \widehat{\mathrm{disc}}(T, S_i)$, compute the optimal weights $\boldsymbol{\alpha}^*(h)$ using Eq. (7) and temperature τ

7: Compute the objective value $U_h = \langle \widehat{\mathbf{g}}_h, \boldsymbol{\alpha}^*(h) \rangle + \tau \|\boldsymbol{\alpha}^*(h)\|_2$ and take a gradient step $h \leftarrow h - \eta \frac{\partial U_h}{\partial h}$

8: **until** convergence

9: **return** h

[2] For example, if $\mathbf{z}$ are the logits of the final classification layer of a neural network, this projection provides another way to produce class probabilities similar to the softmax transformation.

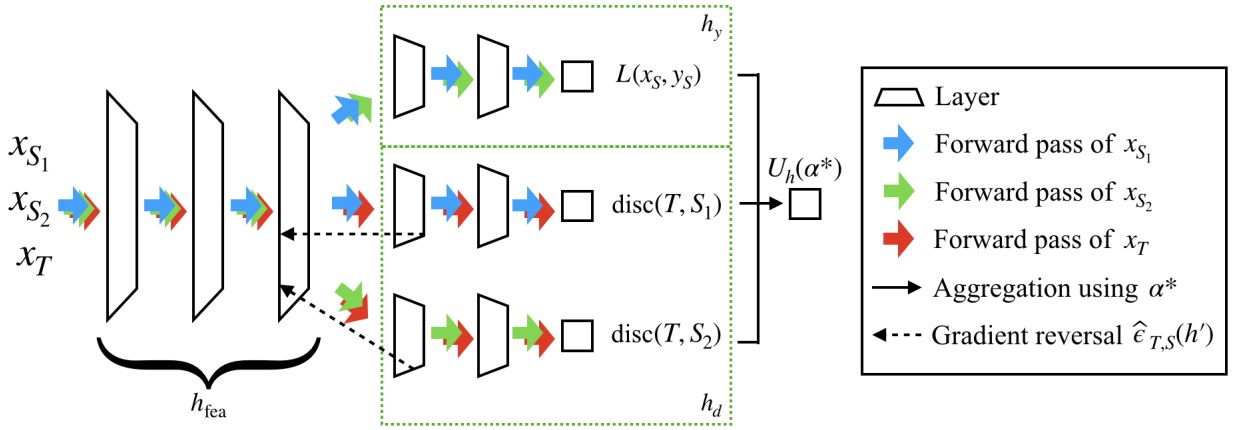

Figure 2: DARN architecture with two source domains (best viewed in color). Mini-batches of x_{S_i} and x_T are fed to the network. x_{S_i} will go through the classification/regression path on the upper h_y box, while all x will go through to the corresponding discrepancies (in the lower h_d box). The gradients from the discrepancies will be reverted during backpropagation.

3.3. Complexity Analysis

Here we analyze the time and space complexities of the algorithm in each iteration. Similar to MDAN (Zhao et al., 2018), in each gradient step, we need to compute the task loss $\mathcal{L}_{\widehat{S}_i}(h, f_{S_i})$ and the $\text{disc}(T, S_i)$ (or $d_{\mathcal{A}}$-distance) using mini-batches from each source domain $i \in [k]$. The question is whether one can maintain the $O(k)$ complexity given that we need to compute the weights using Eq. (7) and backprop through it. For the forward computation of $\boldsymbol{\alpha}^*$, in order to compute the threshold ν^* to the $\epsilon > 0$ relative precision, the binary search will cost $O(k \log(1/\epsilon))$. As for the backward pass of gradient computation, according to our calculation in Appendix B, the Jacobian $J = \partial \boldsymbol{\alpha} / \partial \mathbf{z}$ has a concise form, meaning that it is possible to compute the matrix-vector product $J\mathbf{v}$ for a given vector $\mathbf{v}$ in $O(k)$ time and space. Therefore, our space complexity is the same as MDAN and our time complexity is slightly slower by a factor of $\log(1/\epsilon)$. In comparison, the time complexity for MDMN (Li et al., 2018) is $O(k^2)$ because it requires computing the pairwise weights within the k source domains. When there are a lot of source domains, MDMN will be noticeably slower than MDAN and DARN.

4. Related Work

The idea of utilizing data from the source domain (S, f_S) to train a model for a different but related target domain (T, f_T) has been explored extensively for the last decade using different assumptions (Pan & Yang, 2009; Zhang et al., 2015). For instance, the covariate shift setting (Shimodaira, 2000; Gretton et al., 2009; Sugiyama & Kawanabe, 2012; Wen et al., 2014) assumes $S \neq T$ but $f_S = f_T$, while concept drift (Jiang & Zhai, 2007; Gama et al., 2014) assumes $S = T$ but $f_S \neq f_T$. More specifically, both domain discrepancy and hypothesis class contribute to the adaptation performance (Ben-David et al., 2010b).

Finding a domain-invariant feature space by minimizing a distance measure is common practice in domain adaptation, especially for training neural networks. Tzeng et al. (2017) provided a comprehensive framework that subsumes several prior efforts on learning shared representations across domains (Tzeng et al., 2015; Ganin et al., 2016). DARN uses adversarial domain classifier and the gradient reversal trick from Ganin et al. (2016). Instead of proposing a new loss for each pair of the source and target domains, one of our contributions is the aggregation technique of computing the mixing coefficients $\boldsymbol{\alpha}$, which is derived from theoretical guarantees. When dealing with multiple source domains, our aggregation method can certainly be applied to other forms of discrepancies such as MMD (Gretton et al., 2012; Long et al., 2015; 2016), and other model architectures such as Domain Separation Network (Bousmalis et al., 2016), cycle-consistent model (Hoffman et al., 2018b), class-dependent adversarial domain classifier (Pei et al., 2018) and Known Unknown Discrimination (Schoenauer-Sebag et al., 2019).

Our work focuses on multi-source to single-target adaptation, which has been investigated in the literature. Sun et al. (2011) developed a generalization bound but resorted to heuristic algorithms to adjust distribution shifts. Zhao et al. (2018) proposed a certain ad-hoc scheme for the combination coefficients $\boldsymbol{\alpha}$, which, unlike ours, are not theoretically justified. Multiple Domain Matching Network (MDMN) (Li et al., 2018) computes domain similarities not only between the source and target domains but also within the source domain themselves based on Wasserstein-like measure. Calculating such pairwise weights can be computationally de-

manding when we have a lot of source domains. Their bound requires additional smooth assumptions on the labelling functions f_{S_i}, f_T, and is not a finite-sample bound, as opposed to ours. As for the actual algorithm, they also use ad-hoc coefficients $\boldsymbol{\alpha}$ without theoretical justification. Mansour et al. (2009b;c) consider multi-source adaptation where $T = \sum_i \beta_i S_i$ is a convex mixture of source distributions with some weights β_i. Our analysis does not require this assumption. Hoffman et al. (2018a) provides similar guarantees with different assumptions, but unlike ours, their bounds are not finite-sample bounds.

5. Experiments

In this section, we demonstrate some of the key properties of DARN on a synthetic regression problem, then compare DARN to several state-of-the-art methods on multiple challenging real-world tasks. Additional experiment details can be found in Appendix C.

5.1. Regression on Synthetic Data

Setup. We construct eight source domains that evenly cover the sin function on $[-\pi, \pi]$ (see Fig. 3a). Similarly, we construct four target domains on the same region (see Fig. 3b). Each source/target domain has 100 data points.

We use labelled source data and unlabelled target data for learning. We take on one target domain at a time, and learn a linear model from *all* eight source domains with MSE loss. The goal is to see whether DARN can focus on the relevant source domains and learn a linear model that can perform well on the target domain.

Results and Analysis. First, Fig. 3b shows the learned models. The linear models can fit the target data very well. This shows that DARN can learn a meaningful model for a specific target domain, using only labelled source data and unlabelled target data. Second, Fig. 3c shows the source domain weights (the $\boldsymbol{\alpha}$) for each target domain after training. The weight colors correspond to the colors in Fig. 3a. Noticeably DARN can focus well on the respective relevant source domains for each target domain and ignore the rest. Note that these domain weights are automatically learned during the training of the model.

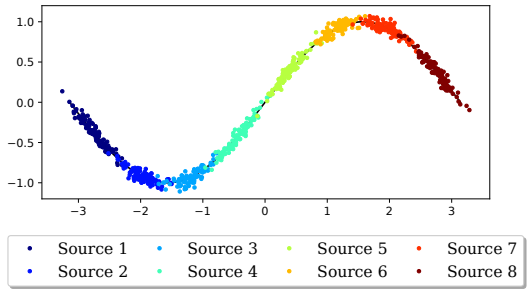

(a) Source domains

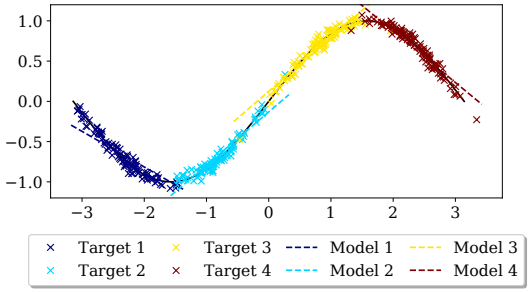

(b) Target domains & learned models

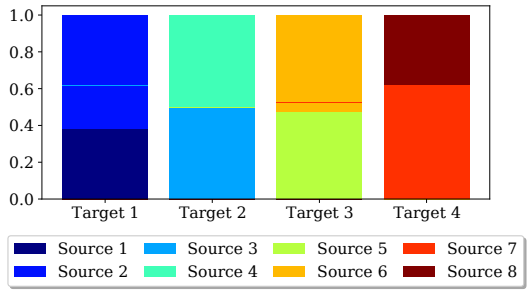

(c) Domain weights ($\boldsymbol{\alpha}$ values)

Figure 3: Regression experiment (best viewed in color).

5.2. Digit Recognition

Setup. Following previous works (Ganin et al., 2016; Zhao et al., 2018), we use the four digit recognition datasets in this experiment (MNIST, MNIST-M, SVHN and Synth). MNIST is a well-known gray-scale images for digit recognition, and MINST-M (Ganin & Lempitsky, 2015) is a variant where the black and white pixels are masked with color patches. Street View House Number (SVHN) (Netzer et al., 2011) is a standard digit dataset taken from house numbers in Google Street View images. Synthetic Digits (Synth) (Ganin & Lempitsky, 2015) is a synthetic dataset that mimic SVHN using various transformations. One of the four datasets is chosen as unlabelled target domain in turn and the other three are used as labelled source domains.

Baselines. We compare DARN to several baselines and state-of-the-art methods. There are many approaches in the literature dealing with single-source to single-target adaption. Since our focus is on the *multi-source* setting, we mainly compare DARN to the most relevant methods that utilize multiple sources for adaptation. (1) The **SRC** (for source) method uses only labelled source data to train the model. It merges all available source examples to form a large dataset to perform training without adaptation. (2) **TAR** (for target) is another baseline that only uses labelled target data. It serves as performance upper

Table 1: Classification accuracy (%) of the target digit datasets. Mean and standard error over 20 runs. The best method (excluding TAR) based on one-sided Wilcoxon signed-rank test at the 5% significance level is shown in bold for each domain.

Method	MNIST	MNIST-M	SVHN	Synth	Avg.
SRC	96.78 ± 0.08	60.80 ± 0.21	68.99 ± 0.69	84.09 ± 0.27	77.66 ± 0.14
DANN	96.41 ± 0.13	60.10 ± 0.27	70.19 ± 1.30	83.83 ± 0.25	77.63 ± 0.35
M3SDA	96.95 ± 0.06	65.03 ± 0.80	71.66 ± 1.16	80.12 ± 0.56	78.44 ± 0.36
MDAN	97.10 ± 0.10	64.09 ± 0.31	77.72 ± 0.60	85.52 ± 0.19	81.11 ± 0.21
MDMN	97.15 ± 0.09	64.34 ± 0.27	76.43 ± 0.48	85.80 ± 0.21	80.93 ± 0.16
DARN	**98.09** ± 0.03	**67.06** ± 0.14	**81.58** ± 0.14	**86.79** ± 0.09	**83.38** ± 0.06
TAR	99.02 ± 0.02	94.66 ± 0.10	87.40 ± 0.17	96.90 ± 0.09	94.49 ± 0.07

bound as if we had access to the true label of the target data. (3) Domain Adversarial Neural Network (**DANN**) (Ganin et al., 2016) is similar to our method in that we both use adversarial training objectives. Here we follow the previous protocol (Zhao et al., 2018) and merge all source data to form a large joint source dataset of km instances for DANN. (4) Moment Matching for Multi-Source Domain Adaptation (**M3SDA**) (Peng et al., 2019) is a recent state-of-the-art method that combines moment matching and maximizing classifier discrepancy (Saito et al., 2018). We use their public code with a few necessary adjustments (change classification head based on the number of classes etc.) (5) Multisource Domain Adversarial Network (**MDAN**) (Zhao et al., 2018) resembles our method in that we both dynamically assign each source domain an importance weight during training. However, unlike ours, their weights are not theoretically justified. We use the soft version from their code since it is reported to perform better than the hard version. (6) Multiple Domain Matching Network (**MDMN**) (Li et al., 2018) computes weights not only between source and target domains but also within source domain themselves. We use their code of computing weights in our implementation. All the methods are applied to the same neural network structure to ensure fair comparison.

Results and Analysis. Table 1 shows the classification accuracy of each target dataset. The last column is the average accuracy of four domains, and the standard errors are calculated based on 20 runs. (1) Most methods can consistently outperform SRC, which has no adaptation. This shows the improvement when using unlablelled target data for adaptation. (2) Without proper weighting for each source domain, DANN with joint source data can sometimes perform worse than SRC. This suggests the importance of ignoring irrelevant data to avoid negative transfer. (3) DARN significantly outperforms other methods across all four domains, especially on the MNIST-M and SVHN domains. Notice that even though MDAN and MDMN have generalization guarantees, they both resort to ad-hoc aggregation rules to combine the source domains during training. Instead, our aggregation (Eq. (7)) is a direct optimization of the upper bound (Theorem 2) thus is theoretically justified and empirically superior for this problem.

5.3. Object Recognition: Office-Home

Setup. To show the applicability of our method to more complicated real-world tasks, we use the challenging Office-Home dataset (Venkateswara et al., 2017). It contains images of 65 classes such as spoon, sink, mug and pen from four different domains: Art, Clipart, Product and Real-World. One of the four datasets is chosen as unlabelled target domain in turn and the other three are used as labelled source domains.

Results and Analysis. Table 2 shows the classification accuracy of each target dataset over 20 runs. Most existing works in the literature focused on single-source adaptation for this problem (e.g., see Long et al. (2018)). Compared to them, using multi-source methods can significantly boost performance, revealing the importance of properly combining multiple source domains. Even though this is a significantly more challenging problem with more classes and much fewer images compared to the digit datasets, DARN achieves state-of-the-art performance in this setting, excelling existing methods by a noticeable margin.

5.4. Sentiment Analysis

Setup. We use the Amazon review dataset (Blitzer et al., 2007; Chen et al., 2012) that consists of positive and negative product reviews from four domains (Books, DVD, Electronics and Kitchen). Each of them is used in turn as the target domain and the other three are used as source domains. We follow the common protocol (Chen et al., 2012; Zhao et al., 2018) of using the top-5000 frequent unigrams/bigrams of all reviews as bag-of-words features.

Results and Analysis. Table 3 summarizes the classification accuracies over 20 runs. (1) Some domains are harder to adapt to than the others. For example, the accuracies of

Table 2: Classification accuracy (%) of the Office-Home datasets. Mean and standard error over 20 runs. The best method (excluding TAR) based on one-sided Wilcoxon signed-rank test at the 5% significance level is shown in bold for each domain.

Method	Art	Clipart	Product	Real-World	Avg.
SRC	58.02 ± 0.47	57.29 ± 0.30	74.26 ± 0.22	77.98 ± 0.25	66.89 ± 0.16
DANN	57.39 ± 0.69	57.35 ± 0.35	73.78 ± 0.27	78.12 ± 0.21	66.66 ± 0.19
M3SDA	64.05 ± 0.61	62.79 ± 0.37	76.21 ± 0.30	78.63 ± 0.22	70.42 ± 0.18
MDAN	68.14 ± 0.58	67.04 ± 0.21	81.03 ± 0.22	82.79 ± 0.15	74.75 ± 0.18
MDMN	68.67 ± 0.55	67.75 ± 0.20	81.37 ± 0.18	83.32 ± 0.14	75.28 ± 0.15
DARN	**70.00** ± 0.38	**68.42** ± 0.14	**82.75** ± 0.21	**83.88** ± 0.16	**76.26** ± 0.13
TAR	71.19 ± 0.38	79.16 ± 0.16	90.66 ± 0.15	85.60 ± 0.14	81.65 ± 0.12

Table 3: Classification accuracy (%) of the target sentiment datasets. Mean and standard error over 20 runs. The best method(s) (excluding TAR) based on one-sided Wilcoxon signed-rank test at the 5% significance level is(are) shown in bold for each domain.

Method	Books	DVD	Electronics	Kitchen	Avg.
SRC	79.15 ± 0.39	80.38 ± 0.30	85.48 ± 0.10	85.46 ± 0.34	82.62 ± 0.20
DANN	79.13 ± 0.29	80.60 ± 0.29	85.27 ± 0.14	85.56 ± 0.28	82.64 ± 0.14
M3SDA	79.42 ± 0.17	80.82 ± 0.35	85.52 ± 0.19	86.45 ± 0.43	83.05 ± 0.14
MDAN	**79.99** ± 0.20	**81.66** ± 0.19	84.76 ± 0.17	86.82 ± 0.13	83.31 ± 0.08
MDMN	**80.13** ± 0.20	**81.58** ± 0.21	85.61 ± 0.13	**87.13** ± 0.11	**83.61** ± 0.07
DARN	**79.93** ± 0.19	**81.57** ± 0.16	**85.75** ± 0.16	**87.15** ± 0.14	**83.60** ± 0.08
TAR	84.10 ± 0.13	83.68 ± 0.12	86.11 ± 0.32	88.72 ± 0.14	85.65 ± 0.09

SRC and TAR on the Electronics domain are very close to each other, indicating that this requires little to no adaptation. Yet, DARN is the closest to the TAR performance here. The Books domain is more challenging. Even though there exists a large gap between SRC and TAR, the improvements over the SRC method are very small for all methods. (3) DARN is always within the best performing methods and significantly outperforms others in the Electronics domain. Note that MDMN additionally computes similarities within source domains in each iteration, which can be computationally expensive ($O(k^2)$ per iteration) if the number of source domains is large. Instead, DARN focuses on the discrepancy between source and target domains ($O(k)$ per iteration) so it is more efficient.

5.5. Visualizing Domain Importance

To show how DARN can aggregate multiple source domains effectively, we visualize the source domain weights (i.e., $\boldsymbol{\alpha}$ in DARN) for the Amazon dataset. We also compared to the weights of MDMN, using the original authors' code.

Fig. 4 and Fig. 5 compare the evolution of source domain weights during training. In each subfigure, every row corresponds to the weights of the source domains when learning for one target domain. Brighter color indicates larger weight and the target domain itself has no weight. They are evaluated at the end of each epoch over 50 epochs. To avoid noisy values due to small mini-batch size, the values are exponential moving averages with a decay rate of 0.95. There are a few observations. (1) The domain weights produced by MDMN are not very stable. We can see that their weights change drastically, especially towards the end of the training (e.g., epochs 40-50 for the Books target domain). After examining the MDMN weights, we notice that it can produce alternating *one-hot* vectors $\boldsymbol{\alpha}$, constantly changing from one domain to a different domain and ignoring the rest. This instability makes their domain weights hard to interpret. (2) In comparison, DARN has smoother weights during training. In Fig. 5, as Electronics and Kitchen are more related to each other than Books and DVD, their respective weights remain higher during training. This is reasonable since they have overlapping products (e.g., blenders). (3) The $\boldsymbol{\alpha}$ of DARN is changing dynamically during training, showing the flexibility of DARN to adjust domain importance when necessary.

6. Conclusion and Future Work

This work uses the discrepancy (Mansour et al., 2009a; Cortes et al., 2019) to derive a finite-sample generalization bound for multi-source to single-target adaptation. We show that, in order to achieve the best possible generalization up-

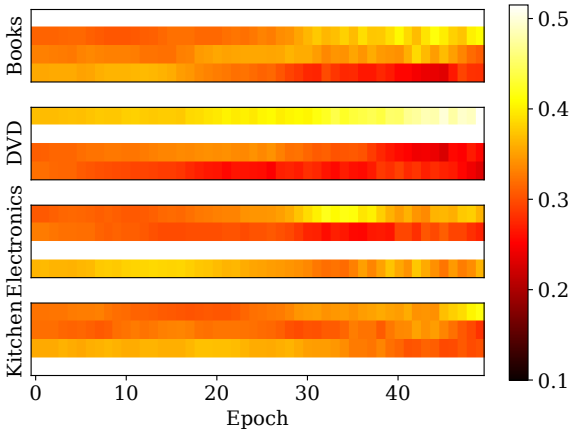

Figure 4: Domain weights of MDMN for the Amazon data.

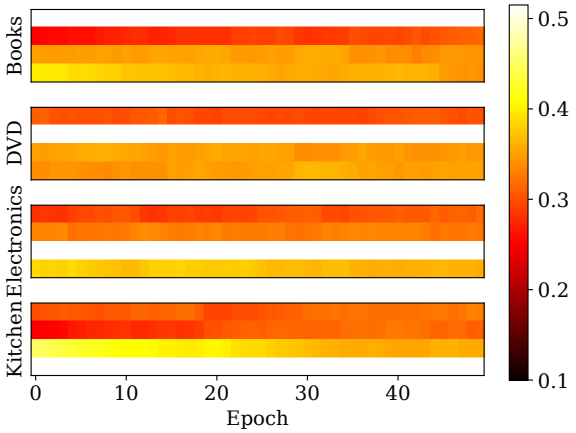

Figure 5: Domain weights of DARN for the Amazon data.

per bound for a target domain, we need to trade-off between including all source domains to increase effective sample size and excluding less relevant domains to avoid negative transfer. Based on the theory, we develop an algorithm, Domain AggRegation Network (DARN), that can dynamically adjust the weight of each source domain during end-to-end training. Experiments on digit/object recognition and sentiment analysis show that DARN outperforms state-of-the-art alternatives. Recent analysis (Zhao et al., 2019; Johansson et al., 2019) show that solely focusing on learning domain invariant features can be insufficient when the marginal label distributions are significantly different. Thus it makes sense to take $\eta_{\mathcal{H}}$ into consideration when a small amount of labelled data is available for the target domain, which we will explore in the future.

Acknowledgements

JW wants to thank Han Zhao for the fruitful discussions. This work is supported by the Alberta Machine Intelligence Institute (Amii).

References

Bartlett, P. L. and Mendelson, S. Rademacher and gaussian complexities: Risk bounds and structural results. *Journal of Machine Learning Research*, 3(Nov):463–482, 2002.

Ben-David, S., Blitzer, J., Crammer, K., and Pereira, F. Analysis of representations for domain adaptation. In *Advances in neural information processing systems*, pp. 137–144, 2007.

Ben-David, S., Blitzer, J., Crammer, K., Kulesza, A., Pereira, F., and Vaughan, J. W. A theory of learning from different domains. *Machine learning*, 79(1-2):151–175, 2010a.

Ben-David, S., Lu, T., Luu, T., and Pál, D. Impossibility theorems for domain adaptation. In *International Conference on Artificial Intelligence and Statistics*, pp. 129–136, 2010b.

Blitzer, J., Dredze, M., and Pereira, F. Biographies, bollywood, boom-boxes and blenders: Domain adaptation for sentiment classification. In *Proceedings of the 45th annual meeting of the association of computational linguistics*, pp. 440–447, 2007.

Blitzer, J., Crammer, K., Kulesza, A., Pereira, F., and Wortman, J. Learning bounds for domain adaptation. In *Advances in neural information processing systems*, pp. 129–136, 2008.

Bousmalis, K., Trigeorgis, G., Silberman, N., Krishnan, D., and Erhan, D. Domain separation networks. In *Advances in Neural Information Processing Systems*, pp. 343–351, 2016.

Bousquet, O., Boucheron, S., and Lugosi, G. Introduction to statistical learning theory. In *Summer School on Machine Learning*, pp. 169–207. Springer, 2003.

Chen, M., Xu, Z., Weinberger, K. Q., and Sha, F. Marginalized denoising autoencoders for domain adaptation. In *Proceedings of the 29th International Coference on International Conference on Machine Learning*, pp. 1627–1634. Omnipress, 2012.

Cortes, C. and Mohri, M. Domain adaptation in regression. In *International Conference on Algorithmic Learning Theory*, pp. 308–323. Springer, 2011.

Cortes, C., Mohri, M., and Medina, A. M. Adaptation based on generalized discrepancy. *The Journal of Machine Learning Research*, 20(1):1–30, 2019.

Duchi, J., Shalev-Shwartz, S., Singer, Y., and Chandra, T. Efficient projections onto the l 1-ball for learning in high dimensions. In *Proceedings of the 25th international conference on Machine learning*, pp. 272–279. ACM, 2008.

Gama, J., Žliobaitė, I., Bifet, A., Pechenizkiy, M., and Bouchachia, A. A survey on concept drift adaptation. *ACM computing surveys (CSUR)*, 46(4):44, 2014.

Ganin, Y. and Lempitsky, V. Unsupervised domain adaptation by backpropagation. In *International Conference on Machine Learning*, pp. 1180–1189, 2015.

Ganin, Y., Ustinova, E., Ajakan, H., Germain, P., Larochelle, H., Laviolette, F., Marchand, M., and Lempitsky, V. Domain-adversarial training of neural networks. *The Journal of Machine Learning Research*, 17(1):2096–2030, 2016.

Goodfellow, I., Pouget-Abadie, J., Mirza, M., Xu, B., Warde-Farley, D., Ozair, S., Courville, A., and Bengio, Y. Generative adversarial nets. In *Advances in neural information processing systems*, pp. 2672–2680, 2014.

Gretton, A., Smola, A., Huang, J., Schmittfull, M., Borgwardt, K., and Schölkopf, B. Covariate shift by kernel mean matching. *Dataset shift in machine learning*, 3(4): 5, 2009.

Gretton, A., Borgwardt, K. M., Rasch, M. J., Schölkopf, B., and Smola, A. A kernel two-sample test. *Journal of Machine Learning Research*, 13(Mar):723–773, 2012.

Hoffman, J., Mohri, M., and Zhang, N. Algorithms and theory for multiple-source adaptation. In *Advances in Neural Information Processing Systems*, pp. 8246–8256, 2018a.

Hoffman, J., Tzeng, E., Park, T., Zhu, J.-Y., Isola, P., Saenko, K., Efros, A., and Darrell, T. Cycada: Cycle-consistent adversarial domain adaptation. In *International Conference on Machine Learning*, pp. 1994–2003, 2018b.

Jiang, J. and Zhai, C. Instance weighting for domain adaptation in NLP. In *Proceedings of the 45th annual meeting of the association of computational linguistics*, pp. 264–271, 2007.

Johansson, F., Sontag, D., and Ranganath, R. Support and invertibility in domain-invariant representations. In *The 22nd International Conference on Artificial Intelligence and Statistics*, pp. 527–536, 2019.

Kifer, D., Ben-David, S., and Gehrke, J. Detecting change in data streams. In *Proceedings of the Thirtieth international conference on Very large data bases-Volume 30*, pp. 180–191. VLDB Endowment, 2004.

Koltchinskii, V., Panchenko, D., et al. Empirical margin distributions and bounding the generalization error of combined classifiers. *The Annals of Statistics*, 30(1): 1–50, 2002.

Li, Y., Carlson, D. E., et al. Extracting relationships by multi-domain matching. In *Advances in Neural Information Processing Systems*, pp. 6798–6809, 2018.

Long, M., Cao, Y., Wang, J., and Jordan, M. Learning transferable features with deep adaptation networks. In *International Conference on Machine Learning*, pp. 97–105, 2015.

Long, M., Zhu, H., Wang, J., and Jordan, M. I. Unsupervised domain adaptation with residual transfer networks. In *Advances in Neural Information Processing Systems*, pp. 136–144, 2016.

Long, M., Cao, Z., Wang, J., and Jordan, M. I. Conditional adversarial domain adaptation. In *Advances in Neural Information Processing Systems*, pp. 1640–1650, 2018.

Mansour, Y., Mohri, M., and Rostamizadeh, A. Domain adaptation: Learning bounds and algorithms. In *22nd Conference on Learning Theory, COLT 2009*, 2009a.

Mansour, Y., Mohri, M., and Rostamizadeh, A. Domain adaptation with multiple sources. In *Advances in neural information processing systems*, pp. 1041–1048, 2009b.

Mansour, Y., Mohri, M., and Rostamizadeh, A. Multiple source adaptation and the Rényi divergence. In *UAI*, pp. 367–374, 2009c.

Netzer, Y., Wang, T., Coates, A., Bissacco, A., Wu, B., and Ng, A. Y. Reading digits in natural images with unsupervised feature learning. In *NIPS Workshop on Deep Learning and Unsupervised Feature Learning 2011*, 2011.

Pan, S. J. and Yang, Q. A survey on transfer learning. *IEEE Transactions on knowledge and data engineering*, 22(10): 1345–1359, 2009.

Pei, Z., Cao, Z., Long, M., and Wang, J. Multi-adversarial domain adaptation. In *Thirty-Second AAAI Conference on Artificial Intelligence*, 2018.

Peng, X., Bai, Q., Xia, X., Huang, Z., Saenko, K., and Wang, B. Moment matching for multi-source domain adaptation. In *Proceedings of the IEEE International Conference on Computer Vision*, pp. 1406–1415, 2019.

Saito, K., Watanabe, K., Ushiku, Y., and Harada, T. Maximum classifier discrepancy for unsupervised domain adaptation. In *Proceedings of the IEEE Conference on Computer Vision and Pattern Recognition*, pp. 3723–3732, 2018.

Schoenauer-Sebag, A., Heinrich, L., Schoenauer, M., Sebag, M., Wu, L., and Altschuler, S. Multi-domain adversarial learning. In *International Conference on Learning Representations*, 2019.

Shimodaira, H. Improving predictive inference under covariate shift by weighting the log-likelihood function. *Journal of statistical planning and inference*, 90(2):227–244, 2000.

Sugiyama, M. and Kawanabe, M. *Machine learning in non-stationary environments: Introduction to covariate shift adaptation*. MIT press, 2012.

Sun, Q., Chattopadhyay, R., Panchanathan, S., and Ye, J. A two-stage weighting framework for multi-source domain adaptation. In *Advances in neural information processing systems*, pp. 505–513, 2011.

Tzeng, E., Hoffman, J., Darrell, T., and Saenko, K. Simultaneous deep transfer across domains and tasks. In *Proceedings of the IEEE International Conference on Computer Vision*, pp. 4068–4076, 2015.

Tzeng, E., Hoffman, J., Saenko, K., and Darrell, T. Adversarial discriminative domain adaptation. In *Proceedings of the IEEE Conference on Computer Vision and Pattern Recognition*, pp. 7167–7176, 2017.

Venkateswara, H., Eusebio, J., Chakraborty, S., and Panchanathan, S. Deep hashing network for unsupervised domain adaptation. In *(IEEE) Conference on Computer Vision and Pattern Recognition (CVPR)*, 2017.

Wen, J., Yu, C.-N., and Greiner, R. Robust learning under uncertain test distributions: Relating covariate shift to model misspecification. In *ICML*, pp. 631–639, 2014.

Zhang, K., Gong, M., and Schölkopf, B. Multi-source domain adaptation: A causal view. In *Twenty-ninth AAAI conference on artificial intelligence*, 2015.

Zhao, H., Zhang, S., Wu, G., Moura, J. M., Costeira, J. P., and Gordon, G. J. Adversarial multiple source domain adaptation. In *Advances in Neural Information Processing Systems*, pp. 8559–8570, 2018.

Zhao, H., Des Combes, R. T., Zhang, K., and Gordon, G. On learning invariant representations for domain adaptation. In *International Conference on Machine Learning*, pp. 7523–7532, 2019.

Appendix

A. Proof of Theorem 2

Theorem 2 *Given k source domains datasets $\{(x_j^{(i)}, y_j^{(i)}) : i \in [k], j \in [m]\}$ with m iid examples each where $\widehat{S}_i = \{x_j^{(i)}\}$ and $y_j^{(i)} = f_{S_i}(x_j^{(i)})$, for any $\boldsymbol{\alpha} \in \Delta = \{\boldsymbol{\alpha} : \alpha_i \geq 0, \sum_i \alpha_i = 1\}, \delta \in (0,1)$, and $\forall h \in \mathcal{H}$, w.p. at least $1-\delta$*

$$\mathcal{L}_T(h, f_T) \leq \sum_i \alpha_i \left[\mathcal{L}_{\widehat{S}_i}(h, f_{S_i}) + \operatorname{disc}(T, S_i) + 2\mathfrak{R}_m(\mathcal{H}_{S_i}) + \eta_{\mathcal{H},i}\right] + \|\boldsymbol{\alpha}\|_2 M_S \sqrt{\frac{\log(1/\delta)}{2m}},$$

where $\mathcal{H}_{S_i} = \{x \mapsto L(h(x), f_{S_i}(x)) : h \in \mathcal{H}\}$ is the set of functions mapping x to the corresponding loss, $\eta_{\mathcal{H},i}$ is a constant similar to Eq. (3) with $\widehat{Q} = \widehat{S}_i$, $\widehat{P} = \widehat{T}$ and $M_S = \sup_{i\in[k], x\in\mathcal{X}, h\in\mathcal{H}} L(h(x), f_{S_i}(x))$ is the upper bound on loss on the source domains.

Proof: Given $\boldsymbol{\alpha} \in \Delta$, the mixture $\widehat{S} = \sum_i \alpha_i \widehat{S}_i$ can be considered as the joint source data with km points, where a point $x^{(i)}$ from $\widehat{S}_i$ has weight α_i/m. Define $\Phi = \sup_{h\in\mathcal{H}} \mathcal{L}_T(h, f_T) - \sum_i \alpha_i \mathcal{L}_{\widehat{S}_i}(h, f_{S_i})$. Changing a point $x^{(i)}$ from $\widehat{S}_i$ will change Φ at most $\frac{M_S \alpha_i}{m}$. Using the McDiarmid's inequality, we have $\Pr(\Phi - \mathbb{E}[\Phi] > \epsilon) \leq \exp\left(-\frac{2\epsilon^2 m}{M_S^2 \|\boldsymbol{\alpha}\|_2^2}\right)$. As a result, for $\delta \in (0,1)$, w.p. at least $1-\delta$, the following holds for any $h \in \mathcal{H}$

$$\mathcal{L}_T(h, f_T) \leq \sum_i \alpha_i \mathcal{L}_{\widehat{S}_i}(h, f_{S_i}) + \mathbb{E}[\Phi] + \|\boldsymbol{\alpha}\|_2 M_S \sqrt{\frac{\log(1/\delta)}{2m}}.$$

Now we bound $\mathbb{E}[\Phi]$. Let $\mathcal{H}_{S_i} = \{x \mapsto L(h(x), f_{S_i}(x)) : h \in \mathcal{H}\}$.

$$\begin{aligned}
\mathbb{E}[\Phi] &= \mathbb{E}_{\widehat{S}}\left[\sup_{h\in\mathcal{H}} \mathcal{L}_T(h, f_T) - \sum_i \alpha_i \mathcal{L}_{\widehat{S}_i}(h, f_{S_i})\right] \\
&\leq \mathbb{E}_{\widehat{S}}\left[\sup_{h\in\mathcal{H}} \sum_i \alpha_i \mathcal{L}_{S_i}(h, f_{S_i}) - \sum_i \alpha_i \mathcal{L}_{\widehat{S}_i}(h, f_{S_i})\right] + \sup_{h\in\mathcal{H}}\left(\mathcal{L}_T(h, f_T) - \sum_i \alpha_i \mathcal{L}_{S_i}(h, f_{S_i})\right) \\
&\leq \mathbb{E}_{\widehat{S}}\left[\sum_i \alpha_i \sup_{h\in\mathcal{H}}\left(\mathcal{L}_{S_i}(h, f_{S_i}) - \mathcal{L}_{\widehat{S}_i}(h, f_{S_i})\right)\right] + \sum_i \alpha_i \sup_{h\in\mathcal{H}} \left(\mathcal{L}_T(h, f_T) - \mathcal{L}_{S_i}(h, f_{S_i})\right) \\
&= \sum_i \alpha_i \mathbb{E}_{\widehat{S}_i}\left[\sup_{h\in\mathcal{H}}\left(\mathcal{L}_{S_i}(h, f_{S_i}) - \mathcal{L}_{\widehat{S}_i}(h, f_{S_i})\right)\right] + \sum_i \alpha_i \sup_{h\in\mathcal{H}} \left(\mathcal{L}_T(h, f_T) - \mathcal{L}_{S_i}(h, f_{S_i})\right) \\
&\leq 2\sum_i \alpha_i \mathfrak{R}_m(\mathcal{H}_{S_i}) + \sum_i \alpha_i \sup_{h\in\mathcal{H}} \left(\mathcal{L}_T(h, f_T) - \mathcal{L}_{S_i}(h, f_{S_i})\right) \\
&\leq \sum_i \alpha_i \left(2\mathfrak{R}_m(\mathcal{H}_{S_i}) + \operatorname{disc}(T, S_i) + \eta_{\mathcal{H},i}\right).
\end{aligned}$$

where first and second inequalities are using the subadditivity of sup, followed by the equality using the independence between the domains $\{\widehat{S}_i\}$, the second last inequality is due to the standard "ghost sample" argument in terms of the Rademacher complexity and the last inequality is due to Cortes et al. (2019, Proposition 8) for each individual S_i. ■

B. Jacobian

Here we calculate the Jacobian $J_{ij} = \partial\alpha_i/\partial z_j$ for Eq. (7) in the main text:

$$\boldsymbol{\alpha}^* = [\mathbf{z} - \nu^*\mathbf{1}]_+ / \|[\mathbf{z} - \nu^*\mathbf{1}]_+\|_1.$$

In the following, we write $\boldsymbol{\alpha} = \boldsymbol{\alpha}^*, \nu = \nu^*$ to simplify notations. Let $S = \{i : z_i - \nu > 0\}$ be the support of the probability vector $\boldsymbol{\alpha}$. $J_{ij} = 0$ if $i \notin S$ or $j \notin S$ since $\alpha_i = 0$ in the former case while z_j does not contribute to the $\boldsymbol{\alpha}$ in the latter case. Now consider the case $i, j \in S$. Let $K = \|[\mathbf{z} - \nu\mathbf{1}]_+\|_1 = \sum_{j\in S}(z_j - \nu)$. Then $\alpha_i = (z_i - \nu) \cdot \frac{1}{K}$ and

$$\frac{\partial\alpha_i}{\partial z_j} = \left(\delta_{i=j} - \frac{\partial\nu}{\partial z_j}\right) \cdot \frac{1}{K} - \frac{1}{K^2} \cdot \frac{\partial K}{\partial z_j} \cdot (z_i - \nu) = \frac{1}{K}\left(\delta_{i=j} - \frac{\partial\nu}{\partial z_j} - \frac{\partial K}{\partial z_j} \cdot \alpha_i\right), \tag{11}$$

where $\delta_{i=j}$ is the indicator or delta function. Now we compute $\frac{\partial\nu}{\partial z_j}$ and $\frac{\partial K}{\partial z_j}$. By the definition of ν, we know that

$$\begin{aligned}
&\sum_{j\in S}(z_j - \nu)^2 = |S|\nu^2 - 2\nu\sum_{j\in S} z_j + \sum_{j\in S} z_j^2 = 1 \\
\implies\quad &\nu = \frac{\sum_{j\in S} z_j}{|S|} - \frac{\sqrt{A}}{|S|} \quad \text{where} \quad A = \left(\sum_{j\in S} z_j\right)^2 - |S|\left(\sum_{j\in S} z_j^2 - 1\right) \\
\implies\quad &\frac{\partial\nu}{\partial z_j} = \frac{1}{|S|} - \frac{B_j}{|S|\sqrt{A}} \quad \text{where} \quad B_j = \sum_{j'\in S} z_{j'} - |S|z_j
\end{aligned} \tag{12}$$

The first right-arrow is due to the quadratic formula and realizing that $\sum_{j\in S} z_j/|S|$ is the mean of the supported z_j so ν must be smaller than it (i.e., we take $-$ in the $\pm$ of the quadratic formula, otherwise some of the z_j will not be in the support anymore). And

$$\frac{\partial K}{\partial z_j} = 1 - |S| \cdot \frac{\partial\nu}{\partial z_j} = \frac{B_j}{\sqrt{A}}. \tag{13}$$

Plugging Eq. (12) and Eq. (13) in Eq. (11) gives

$$\frac{\partial\alpha_i}{\partial z_j} = \frac{1}{K}\left[\delta_{i=j} - \frac{1}{|S|} + \frac{B_j}{\sqrt{A}} \cdot \left(\frac{1}{|S|} - \alpha_i\right)\right]$$

Note that

$$\frac{B_j}{K} = \frac{\sum_{j'\in S} z_{j'} - |S|z_j}{\sum_{j'\in S}(z_{j'} - \nu)} = \frac{\sum_{j'\in S}(z_{j'} - \nu) + |S|(\nu - z_j)}{\sum_{j'\in S}(z_{j'} - \nu)} = 1 - |S|\alpha_j.$$

Then

$$J_{ij} = \frac{\partial\alpha_i}{\partial z_j} = \frac{1}{K}\left(\delta_{i=j} - \frac{1}{|S|}\right) + \frac{|S|}{\sqrt{A}}\left(\frac{1}{|S|} - \alpha_i\right)\left(\frac{1}{|S|} - \alpha_j\right).$$

In matrix form,

$$J = \frac{1}{K}\left(\mathrm{Diag}(\mathbf{s}) - \frac{\mathbf{s}\mathbf{s}^\top}{|S|}\right) + \frac{|S|}{\sqrt{A}}\left(\frac{\mathbf{s}}{|S|} - \boldsymbol{\alpha}\circ\mathbf{s}\right)\left(\frac{\mathbf{s}}{|S|} - \boldsymbol{\alpha}\circ\mathbf{s}\right)^\top,$$

where $\mathbf{s} = [s_1, \ldots, s_k]^\top$ is a vector indicating the support $s_i = \delta_{i\in S}$ and $\circ$ is element-wise multiplication. More often, we need to compute its multiplication with a vector $\mathbf{v}$

$$J\mathbf{v} = \frac{\mathbf{s}}{K}\circ\left(\mathbf{v} - \frac{\mathbf{s}^\top\mathbf{v}}{|S|}\right) + \frac{|S|}{\sqrt{A}}\left(\frac{\mathbf{s}}{|S|} - \boldsymbol{\alpha}\circ\mathbf{s}\right)\left(\frac{\mathbf{s}}{|S|} - \boldsymbol{\alpha}\circ\mathbf{s}\right)^\top\mathbf{v}.$$

Note that all quantities except A have been computed during the forward pass of calculating Eq. (7). A can be computed in $O(|S|)$ time so the overall computation is still $O(k)$ since $|S| \le k$.

C. Experiment Details

The following provides additional details of the experiments.

C.1. Regression

For the eight source domains, the ith ($i = \{0, 1, \ldots, 7\}$) domain data is generated by $x_i \sim \mathcal{N}(\frac{\pi}{4}i - \frac{7\pi}{8}, 0.2^2)$ and the output is $y = \sin(x) + \epsilon$ where $\epsilon \sim \mathcal{N}(0, 0.05^2)$ is random noise. For the four target domains, the jth ($j = \{0, 1, 2, 3\}$) domain is generated by $x_j \sim \mathcal{N}(\frac{\pi}{2}j - \frac{3\pi}{4}, 0.4^2)$.

C.2. Digit Recognition

MNIST images are resized to 32×32 and represented as 3-channel color images in order to match the shape of the other three datasets. Each domain has its own given training and test sets when downloaded. Their respective training sample sizes are 60000, 59001, 73257, 479400, and the respective test sample sizes are 10000, 9001, 26032, 9553. In each run, 20000 images are randomly sampled from each domain's training set as actual labelled source or unlabelled target training examples, and 9000 images are randomly sampled from each domain's test set as actual test examples for evaluation. The model structure is shown in Fig. 6. There is no dropout and the hyper-parameters are chosen based on cross-validation. It is trained for 50 epochs and the mini-batch size is 128 per domain. The optimizer is Adadelta with a learning rate of 1.0. The soft version of MDAN has an additional parameter $\gamma = 1/\tau$ which is the inverse of our temperature τ. $\gamma = 0.5$ is used for MDAN and $\gamma = 0.1$ for DARN.

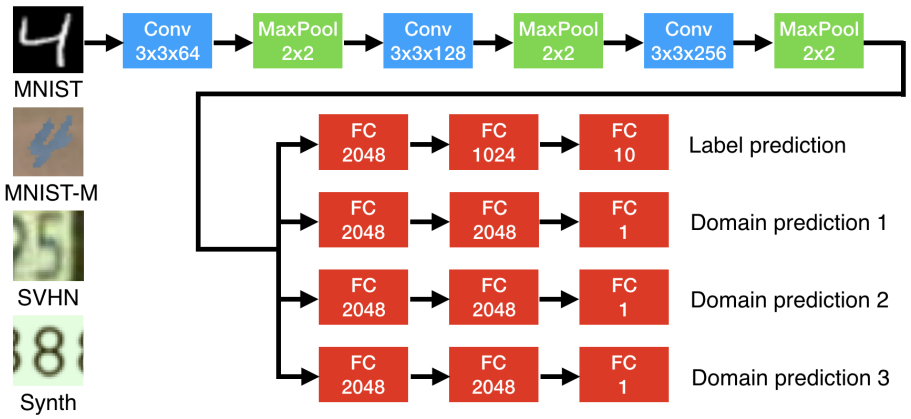

Figure 6: Model architecture for the digit recognition.

C.3. Object Recognition: Office-Home

For the four domains, Art, Clipart, Product and Real-World, the respective sample sizes are 2427, 4365, 4439, 4357. In each run, 2000 images are randomly sampled from each domain as labelled source or unlabelled target training examples, and the rest images are used as test images for evaluation. We use the ResNet50 (He et al., 2016) pretrained features from the ImageNet as the base network for feature learning and put an MLP with [1000, 500, 100, 65] units on top for classification. It is trained for 50 epochs and the mini-batch size is 32 per domain. The optimizer is Adadelta with a learning rate of 1.0. MDAN uses $\gamma = 1.0$ while DARN uses $\gamma = 0.5$.

C.4. Sentiment Analysis

The respective sample sizes for the Books, DVD, Electronics and Kitchen domains are 6465, 5586, 7681, 7945. We train a fully connected model (MLP) with $[1000, 500, 100]$ hidden units for classifying positive versus negative reviews. The dropout drop rate is 0.7 for the input and hidden layers. In each run, we randomly sample 2000 reviews from each domain as labelled source or unlabelled target training examples, while the remaining instances are used as test examples for evaluation. The hyper-parameters are chosen based on cross-validation. The model is trained for 50 epochs and the mini-batch size is 20 per domain. The optimizer is Adadelta with a learning rate of 1.0. The chosen parameters are $\gamma = 10.0$ for MDAN and $\gamma = 0.9$ for our DARN, which are selected from a wide range of candidate values.

Fig. 7 and Fig. 8 show the domain weights of MDMN and DARN *without* exponential average smoothing. They correspond to Fig. 4 and Fig. 5 in the main text. Although both can have certain instability due to small mini-batch size, MDMN is noticeably less stable, especially towards the end of the training, in which alternating one-hot weights can occur (e.g., epochs 40-50 for the Books target domain). This makes their weights hard to interpret.

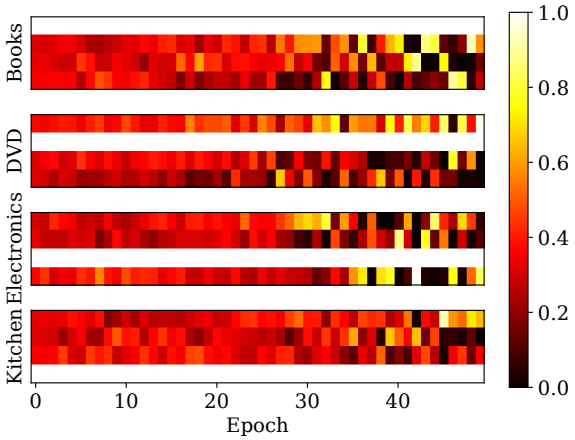

Figure 7: Domain weights of MDMN for the Amazon data.

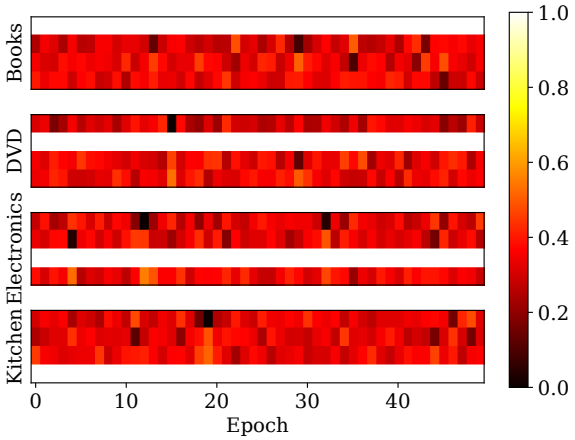

Figure 8: Domain weights of DARN for the Amazon data.